Investigation of the Summer Climate of North America: A Study with a Regional Atmospheric Model
Investigación del Clima del Verano en Norteamérica: Un Estudio con un Modelo Atmosférico Regional

Christopher L. Castro
Department of Atmospheric Science, Colorado State University
Department of Atmospheric Sciences, University of Arizona (July 2006)
E-mail: castro@atmo.arizona.edu

Roger A. Pielke, Sr.
CIRES, University of Colorado at Boulder

Jimmy O. Adegoke
Laboratory for Climate Analysis and Modeling
Department of Geosciences
University of Missouri, Kansas City

1. Introduction

The use of a regional climate model to study the summer weather of North America has many advantages. Global atmospheric models and global reanalyses are currently available for a period greater than fifty years and include large-scale climate variability. However, because of the their low resolution they cannot represent important details like the diurnal cycle of convection, low-level winds that transport moisture toward the continental interior, and the seasonal maximum of rainfall of the North American monsoon. Simulation results with the CSU RAMS model (Δx = 35 km) which use the NCEP-NCAR Global Reanalysis (1950 to 2002) as the lateral boundary condition are presented. In this summary, emphasis is placed on the model climatology and interannual variability associated with remote sea surface temperatures (SSTs).

1. Introducción

El uso de un modelo regional climático para estudiar el tiempo en el verano en Norteamérica tiene muchas ventajas. Actualmente se dispone de modelos atmosféricos globales y de reanálisis globales para un período de más de cincuenta años que incluyen variabilidad climática de gran escala. Sin embargo, debido a la baja resolución no pueden representar detalles importantes como el ciclo diurno de la convección, los vientos de niveles bajos que transportan humedad hacia el interior del continente, y el máximo estacional de lluvia del monzón norteamericano. Se presentan los resultados de simulaciones llevadas a cabo con el modelo RAMS de CSU (Δx = 35 km) utilizando los Reanálisis Globales de NCEP-NCAR (1950 a 2002) como condición límite lateral. En este resumen, se pone énfasis en la climatología del modelo y la variabilidad interanual asociada con las temperaturas superficiales del mar (TSM) en regiones alejadas.

2. Summer Precipitation

2. Precipitación en el Verano

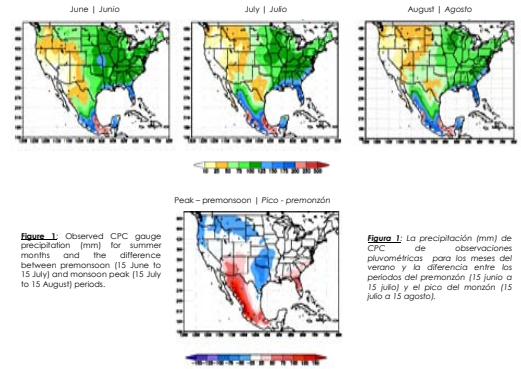

Figure 1: Observed CPC gauge precipitation (mm) for summer months and the difference between premonsoon (15 June to 15 July) and monsoon peak (15 July to 15 August) periods.

***Figura 1**: La precipitación (mm) de CPC de observaciones pluvométricas para los meses del verano y la diferencia entre los períodos del premonzón (15 junio a 15 julio) y el pico del monzón (15 julio a 15 agosto).*

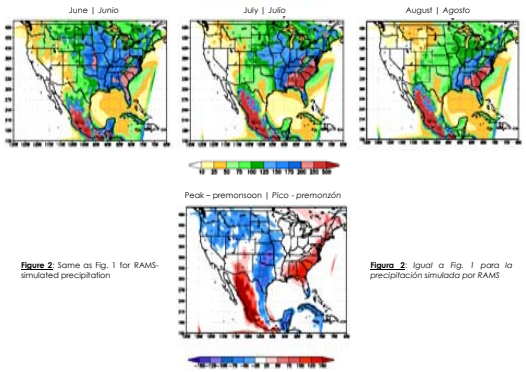

Figure 2: Same as Fig. 1 for RAMS-simulated precipitation

***Figura 2**: Igual a Fig. 1 para la precipitación simulada por RAMS*

The evolution of RAMS-simulated precipitation is reasonable. Prior to monsoon onset there is a rainfall maximum in the central U.S. and a rainfall minimum in the core monsoon region. The development of the monsoon in July and August changes the continental distribution of precipitation, with a dramatic increase in the core monsoon region. The amount of precipitation from the model, in general, is overestimated with respect to gauge observations (a typical result in many models), especially in the southeast U.S. and the Sierra Madre Occidental in Mexico.

La evolución de la precipitación simulada por RAMS es razonable. Antes del inicio del monzón existe un máximo de lluvia en el centro de los EE.UU. y un mínimo de lluvia en la región central del monzón. El desarollo del monzón en julio y agosto cambia la distribución continental de la precipitación, con un aumento dramático en la región central del monzón. La cantidad de precipitación en el modelo, en general, es sobreestimada con respecto a las observaciones pluviométricas (un resultado típico en muchos modelos), especialmente en el sureste de los EE.UU. y en la Sierra Madre Occidental en México.

3. Modes of Convection

RAMS-simulated moisture flux convergence (MFC) is used to investigate time-varying modes of convection. MFC is decomposed using spectral analysis for each year for a moving thirty-day period. The average of all spectra is computed and multiplied by the fraction that is above red noise. Three distinct spectral bands appear, each associated with different rainfall mechanisms.

Synoptic mode (4 to 10 days): Corresponds with surges of moisture from the Gulf of California and the associated passage of upper-level easterly disturbances. Allows convection in the core monsoon region to organize into mesoscale convective complexes that propagate westward from the mountains.

Sub-synoptic mode (1.5 to 3 days): Corresponds with mesoscale convective complexes in the central U.S. that propagate eastward.

Diurnal mode: Corresponds with convection which occurs due to orographic forcing and land-sea contrast. Is the dominant, and the most important, mechanism for summer rainfall.

3. Modos de la Convección

La convergencia del flujo de humedad (CFH) simulada por RAMS se usa para investigar los modos de la convección que varían temporalmente. La CFH se descompone usando análisis espectral para cada año para períodos de treinta días móvil. Se calcula el promedio de todos los espectros y se multiplica por la fracción por encima del ruido rojo. Aparecen tres bandas espectrales en particular, cada una asociada con mecanismos diferentes de lluvia.

Modo sinóptico (4 a 10 días): Corresponde a las oleadas de humedad desde el Golfo de California y el paso asociado de perturbaciones de los niveles-altos del este. Permiten que la convección en la región central del monzón se organice en complejos convectivos de mesoescala que se propagan desde las montañas hacia el oeste.

Modo sub-sinóptico (1.5 a 3 días): Corresponde a los complejos convectivos de mesoescala en el centro de los EE.UU. que se propagan hacia el este.

Modo diurno: Corresponde a la convección que occurre a causa del forzante orográfico y el contraste entre la tierra y el mar. Es el mecanismo dominante, y el más importante, para las lluvias de verano.

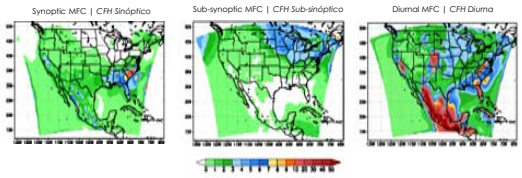

Figure 3: Weighted spectral power of RAMS-simulated July MFC (mm² day⁻²) for the three distinct spectral bands.

***Figura 3**: Energía espectral pesada de la CFH en Julio (mm² day⁻²) en las simulaciones con RAMS para las tres bandas particulares.*

4. Global SST Patterns

To investigate interannual climate variability in the RAMS simulations, the dominant patterns of summer global SST and their associated time series were determined using a rotated principal component analysis. SST modes 1 and 3 are centered in the Pacific and strongly govern North American summer climate. SST mode 1 is ENSO and varies on a timescale between 2 to 5 years. SST mode 3 is probably related to the Pacific Decadal Oscillation. SST mode 2 reflects an increase in tropical SST since 1980 which could be a climate change signal. These modes were also determined to be statistically significant in time using multispectral singular value decomposition analysis.

4. Patrones Globales de la TSM

Para investigar la variabilidad interanual del clima en las simulaciones con RAMS, los patrones dominantes de la TSM global en el verano y las series del tiempo asociadas fueron determinados usando un análisis de componentes principales rotados. Los modos 1 y 3 de la TSM están centrados en el Pacífico y gobieman marcadamente el clima del verano en Norteamérica. El modo 1 de la TSM es el ENSO y varía en una escala temporal entre 2 a 5 años. Es probable que el modo 3 de la TSM esté relacionado con la Oscilación Pacífica Decádica. El modo 2 de la TSM refleja un aumento de la TSM tropical desde 1980 que podría ser una señal del cambio climático. Usando un análisis de descomposición singular multispectral del valor se determinó que estos modos también son estadísticamente significativos en el tiempo.

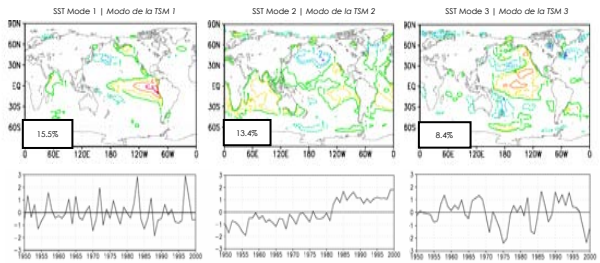

Figure 4: The first three global summer SST modes (1950 to 2000) and their associated normalized time series. The units for SST patterns are arbitrary. The percent explained variance of each mode is also shown.

***Figura 4**: Los primeros tres modos globales de la TSM (1950 a 2000) y las series normlizadas en el tiempo. Las unidades de los patrones de la TSM son arbitrarias . Se muestra también el porcentaje de la variación para cada modo.*

5. Summer Teleconnections

Years are grouped according to the dominant SST modes in the Pacific using composite analysis. Specific and significant patterns in the geopotential height are associated with the SST modes in the Pacific. These patterns evolve in time and are predominant at the beginning of the summer. At that time, the position and intensity of the monsoon ridge is modulated. When the upper-level winds in the Pacific diminish at the end of July, the source of Rossby waves also diminishes and the teleconnections cease.

5. Teleconecciones en el Verano

Los años se agrupan según los modos dominantes de la TSM usando análisis de composición. Patrones particulares y significativos en el geopotencial están asociados con los modos de la TSM en el Pacífico. Estos patrones evolucionan en el tiempo y son predominantes al principio del verano. En ese momento, la posición e intensidad del eje de alta presión del monzón se modifican. Cuando los vientos de niveles altos en el Pacífico disminuyen al final de julio, la fuente de las ondas de Rossby también disminuye y las teleconecciones cesan.

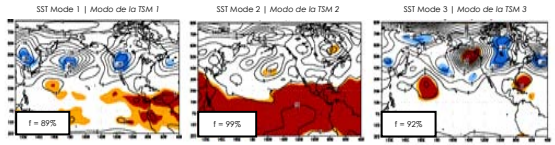

Figure 5: 500-hPa geopotential height anomalies (m) associated with global summer SST modes at the beginning of July. Areas of Local significance shaded at 90% and 95% levels. Field significance (f) also is shown.

***Figura 5**: Anomalías del geopotencial en 500-hPa (m) asociadas con los modos globales de la TSM en el verano, a principios de julio. Se sombrean las áreas significativas locales para los niveles de 90% y 95%. Se muestra también la significancia del mapa (f).*

6. Model Interannual Variability

The teleconnections associated with the interannually varying global SST modes accelerate or delay the onset of the monsoon. This explains the well-known opposite relationship in summer rainfall between the central U.S. and core monsoon region. The recent increase in tropical SST is associated with an increase in summer rainfall in the U.S. and eastern Mexico. However, the model results indicate that summer rainfall in western Mexico decreased over the last twenty years. The same trends also exist in gauge observations. The interannual variability of diurnal MFC shows that the continental divide clearly separates regions with different relationships between precipitation and remote SST.

6. Variabilidad Interanual en el Modelo

Las teleconecciones asociadas con los modos de la TSM global que varían interanualmente aceleran o retrasan el inicio del monzón. Esto explica la relación opuesta bien conocida en la precipitación entre el centro de los EE.UU. y la región central del monzón. El aumento reciente en la TSM tropical está asociado con un aumento de la precipitación en el verano en los EE.UU. y en el este de México. Sin embargo, los resultados del modelo indican que la precipitación en el verano en el oeste de México disminuyó durante los últimos viente años. Las mismas tendencias también existen en las observaciones pluviométricas. La variabilidad de la CFH muestra que la divisoria continental separa claramente las regiones con relaciones diferentes entre la precipitación y la TSM en regiones alejadas.

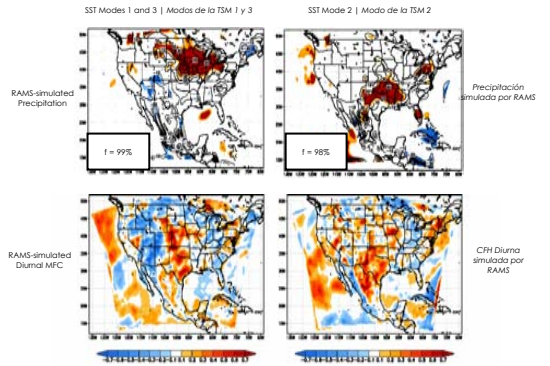

Figure 6: RAMS-simulated precipitation anomalies (mm) and the percentage change in RAMS-simulated diurnal MFC associated with global SST modes. On the precipitation maps, areas of local significance are shaded at the 90% and 95% levels and the field significance (f) is also shown.

***Figura 6**: Las anomalías de la precipitación (mm) simuladas por RAMS y el cambio en el porcentaje de la CFH simulada por RAMS asociados con los modos globales de la TSM. En los mapas de la precipitación, se sombrean las áreas significativas locales para los niveles de 90% y 95% y se muestra también la significancia del mapa (f).*

Acknowledgments: Research funded by NOAA grant NA67RJ0152 and NASA grant NGT5-30344. The authors thank Dr. Adriana Beltrán-Przekurat for assistance in Spanish language translation.

Statistical Characterization of the Spatiotemporal Variability of Soil Moisture and Vegetation in North America for Regional Climate Model Applications

Christopher L. Castro
Department of Atmospheric Sciences, University of Arizona
E-mail: castro@atmo.arizona.edu

Adriana Beltrán-Przekurat and Roger A. Pielke, Sr.
CIRES, University of Colorado at Boulder

The First Climate Prediction Program for the Americas PIs Meeting, Tucson, Arizona, August 14-16, 2006.

1. Introduction

Our previous work has established that the dominant modes of Pacific sea surface temperatures (SSTs) influence the summer climate of North America via remote forcing of the large-scale circulation, or teleconnections. These teleconnections evolve in time and are most apparent during the early part of the summer, affecting the onset of the North American monsoon and the end to the late spring wet period in the central U.S. Our companion poster presented at this meeting summarizes how these teleconnections affect the physical mechanisms of summer rainfall within a regional climate model (RCM) framework. It has also been established via RCMs that the land surface influences of soil moisture and vegetation may significantly impact summer climate. However, these sensitivity-type studies have focused on only one or a few years, typically with extreme climate conditions like 1988 and 1993. The hypothesis posed here is that the land surface influences become more important during the latter part of the summer, when the influence of remote Pacific SST forcing diminishes. Our goal is to eventually test this hypothesis using a RCM as a complement to our previous work, with idealized land surface forcing corresponding to the statistically significant spatiotemporal patterns of soil moisture and vegetation. These must necessarily be "integrators" of longer-term atmospheric variability and may act synergistically with the summer teleconnections to create extreme climate conditions. The results presented herein show our initial statistical analysis of long-term North American precipitation, soil moisture and vegetation greenness datasets. The latter two products will be used to drive future idealized RCM simulations with the Regional Atmospheric Modeling System (RAMS).

2. Description of Soil Moisture and Vegetation Datasets

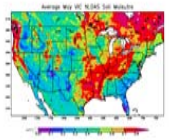

Figure 1: Climatological May soil moisture (unitless value as a fraction of saturation) from VIC model simulations.

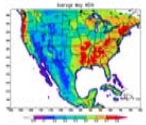

Figure 2: Climatological May NDVI (unitless) derived from AVHRR satellite data.

Soil moisture data is from a long-term integration of the Variable Infiltration Capacity (VIC) hydrologic model over the North American Land Data Assimilation System (NLDAS) domain at one-eighth degree resolution.

Vegetation greenness is defined using the Normalized Difference Vegetation Index (NDVI), available from GIMMS-NDVI data from 1981-present at 8 km resolution (Tucker et al. 2005). NDVI can be used to derive leaf area index (LAI) per RCM vegetation type with a transfer algorithm.

3. Statistical Analysis Methods

MTM-SVD Analysis: Allows for the detection and reconstruction of quasi-oscillatory spatio-temporal climate signals that exhibit episodes of spatially correlated behavior. Produces: 1) a local fractional variance (LFV) spectrum of the principal eigenmode; 2) statistical confidence intervals for the LFV spectrum; and 3) reconstructed anomaly patterns corresponding to the significant time-varying modes (e.g. Rajagopalan et al. 1998). The reference point for soil moisture and vegetation anomalies is defined as being in the central U.S. for the present analysis, unless otherwise specified.

Wavelet Analysis: Decomposes a time series into time/frequency space simultaneously, providing information on periodic signals and how these vary in time (Torrence and Compo 1998). Used here to confirm MTM-SVD analysis results by another method.

4. Dominant Spatiotemporal Modes of Global SST

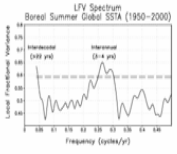

Figure 3: Principal eigenmode LFV spectrum of boreal summer global SST for 1950-2000. Dashed line indicates statistical significance at the 99% level. From Castro et al. (2006).

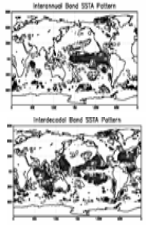

Figure 4: In-phase normalized SSTA associated with interannual and interdecadal bands, referenced to the eastern tropical Pacific. Values greater (less) than 1 (-1) shaded dark (light). Contour interval 0.25 units. From Castro et al. (2006).

Two statistically significant spatiotemporal modes of global SST are related to ENSO and ENSO-like decadal variability in the Pacific, at time scales of 3-4 years and about 22 years, respectively. The patterns shown here are for boreal summer, as this is the season that is of interest in our present work. These SST patterns are related to distinct atmospheric teleconnections in both warm and cold seasons, as shown for example on our companion poster and Castro et al. (2006). We therefore expect a priori that the statistically significant patterns of rainfall, soil moisture, and vegetation greenness would reflect the combination of SST forcing from both of these modes.

5. Standardized Precipitation Index (SPI)

The standardized precipitation index (SPI; McKee et al. 1993) normalizes a given precipitation total at each point to a gamma distribution, allowing for comparison of precipitation anomalies over varying climate regimes on a continental scale. In the present analysis, the one-month SPI is used for the CPC U.S.-Mexico long-term gauge-derived dataset (Higgins et al. 1996) for the period 1950-2002. The LFV spectrum for SPI considering all seasons (Fig. 5) shows significant interannual variability at a timescale of about seven years, which is the band of greatest interest here because significant variability in soil moisture and vegetation greenness occur at approximately the same time scale. This makes sense given that the most coherent patterns of atmospheric forcing, for both cold and warm seasons, occur when the interannual and interdecadal variability in the Pacific are in phase. The spatial pattern of variability reflects the well-established relationships between North American winter precipitation and ENSO/PDO in winter (Fig. 6). The corresponding wavelet analysis (Fig. 7) shows that the longer-term variability in central U.S. SPI is more dominant during the early part of the record and occurs at a slightly lower frequency.

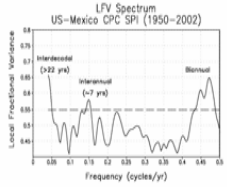

Figure 5: Principal eigenmode LFV spectrum of SPI for CPC U.S.-Mexico precipitation data (1950-2002). Dashed line indicates statistical significance at the 95% level.

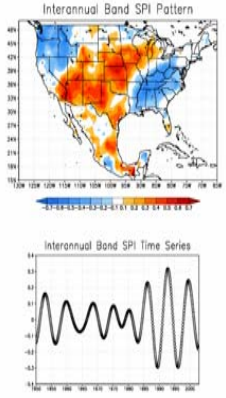

Figure 6: Spatial pattern (top) and time series (bottom) of in-phase SPI in the interannual band (unitless) referenced to the central U.S. for the period 1950-2002.

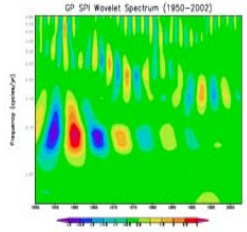

Figure 7: Wavelet spectrum of SPI (unitless) for an area encompassing the Great Plains for the period 1950-2002.

5. SPI Cold vs. Warm Season

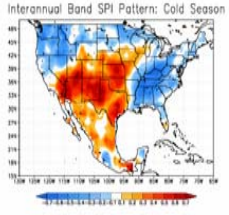

Figure 8: Same as Fig. 6 considering only the cold season (September to May).

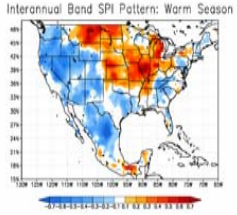

Figure 9: Same as Fig. 6 considering only the warm season (June to August).

A similar analysis of SPI in the interannual band considering total precipitation of the cold season (Fig. 8; September to May) and warm season (Fig. 9; June to August) separately reveals several additional important features of interannual precipitation variability. The cold season SPI pattern mirrors that for all seasons (Fig. 6), indicating that winter precipitation is likely more important than summer precipitation in determining drought conditions on interannual timescales. Central U.S. precipitation anomalies associated with interannual precipitation variability vary in the same way throughout the year. Therefore, the climate extremes in this region are very sensitive to the large-scale atmospheric forcing provided by Pacific SSTs. The most dramatic seasonal shift in the sign of precipitation anomalies associated with interannual variability occurs in the core monsoon region. This reflects the fact that interannual variability in winter versus summer precipitation is inversely related in this region. Therefore, a wet (dry) winter tends to be followed by a dry (wet) monsoon.

6. VIC NLDAS Soil Moisture

The statistically significant mode of interannual variability of VIC NLDAS soil moisture is at a slightly lower frequency than that of the SPI (Fig. 10). The largest anomalies in interannual soil moisture variability occur in the central U.S. (Fig. 11), and this is not surprising because the sign of interannual variation in precipitation there is consistent for the entire year (Figs. 8 and 9). The interannual band time series for soil moisture in the central U.S. (Fig. 11) matches the documented wet and dry periods there very well. In particular, long-term droughts occur at an approximately multidecadal frequency. In the observational record, these include the Dust Bowl of the mid-1930s, mid-1950s, mid-1970s, 1988-89, and the most recent drought of 1998-2002. We hypothesize that the most acute drought conditions in these periods are near the tail end of a cycle of relatively persistent Pacific SSTs, when the soil moisture deficit starts to act synergistically with atmospheric forcing (e.g. 1935-36, 1955-56, 1976-77, 2001-2002).

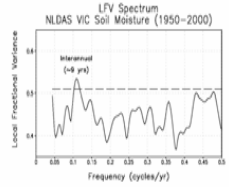

Figure 10: Principal eigenmode LFV spectrum of soil moisture for VIC NLDAS product (1950-2000). Dashed line indicates statistical significance at the 95% level.

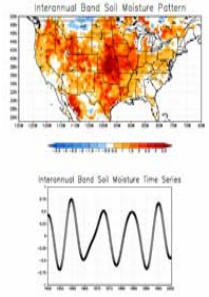

Figure 11: Spatial pattern (top) and time series (bottom) of in-phase VIC soil moisture anomalies in the interannual band (unitless) referenced to the central U.S. for the period 1950-2000.

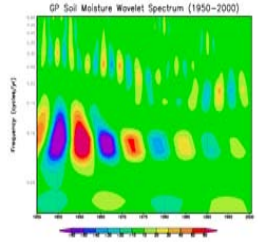

Figure 12: Wavelet spectrum of VIC soil moisture (unitless) for an area encompassing the Great Plains for the period 1950-2000.

7. Satellite-Derived NDVI

Significant interannual variability in AVHRR GIMMS-NDVI occurs on a timescale of about seven years (Fig. 13). Unlike soil moisture, long-term variability in vegetation greenness is a maximum in the southeast U.S. and does not correspond well with precipitation variability (Fig. 14). The likely reason for this is because vegetation growth is influenced by factors other than precipitation in this area. The surface temperature and availability of sunlight, and not moisture availability, may be the more dominant factors. Variability in vegetation greenness in the core monsoon region indicates a dependence on summer rainfall, especially west of the continental divide. We note there is a problem with NDVI data for 1994, which affect the NDVI time-series and wavelet analysis in Figs. 14 and 15. Also, the wavelet analysis is shown for the southeast U.S. instead of the central U.S. in this case.

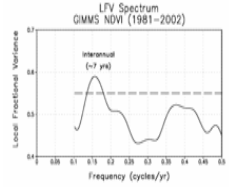

Figure 13: Principal eigenmode LFV spectrum of AVHRR GIMMS-NDVI (1981-2002). Dashed line indicates statistical significance at the 95% level.

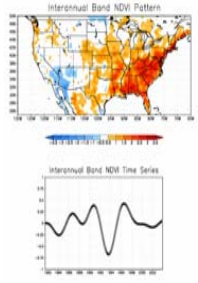

Figure 14: Spatial pattern (top) and time series (bottom) of in-phase AVHRR GIMMS-NDVI in the interannual band (unitless) referenced to the central U.S. for the period 1950-2000.

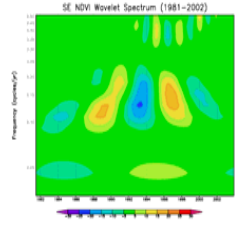

Figure 15: Wavelet spectrum of AVHRR GIMMS-NDVI (unitless) for an area encompassing the southeast U.S. for the period 1950-2000.

Acknowledgments: Research funded by NOAA grant NA67RJ0152 under NOAA CPPA-GAPP.